Val Sorda: An upper Pleistocene loess-paleosol sequence in northeastern Italy

Francesca Ferraro[1,*], Birgit Terhorst[2], Franz Ottner[3], and Mauro Cremaschi[4]

[1]*Earth Science Department, Univ. Milano, via Mangiagalli 34, I-20133 Milano, Italy*
[2]*Institute of Geography, Univ. Tübingen, Hoelderlinstr. 12, D-72074 Tuebingen, Germany*
[3]*Institute of Applied Geology, Univ. Agricultural Sciences Vienna, Peter Jordan Strasse 70, A-1190 Vienna, Austria*
[4]*CNR-IDPA, via Mangiagalli 34, I-20133 Milano, Italy*
* francesca.ferraro@unimi.it

ABSTRACT

The upper Pleistocene loess-paleosol sequence of Val Sorda (northeastern Italy) is investigated with paleopedological, micromorphological, and mineralogical methods. Special emphasis is placed on magnetic parameters and analysis of clay minerals. The base of the sequence is an Eemian paleosol, which consists of a rubefied Bt-horizon formed in till. This Bt-horizon is covered by loess, three interstadial paleosols and colluvial deposits. The three interstadial paleosols have a Chernozem morphology and characteristics, reflecting a dry and continental paleoclimate. The top of the sequence is covered by till deposited during the Solferino Stage glacial advance.

Key words: paleosol, loess, clay minerals, Chernozem, paleoclimate, upper Pleistocene, Val Sorda, Italy.

RESUMEN

La secuencia de paleosuelo de loess del Pleistoceno superior de Val Sorda (Noreste de Italia) ha sido investigada utilizando métodos paleopedológicos, micromorfológicos y mineralógicos. Se ha puesto especial énfasis en parámetros magnéticos y análisis de minerales arcillosos. La base de la secuencia es un paleosuelo del Eemiano, que consiste en un horizonte Bt rubificado formado a partir de till. Este horizonte Bt está cubierto por loess, tres paleosuelos interestadiales y depósitos coluviales. Los tres paleosuelos interestadiales tienen una morfología de Chernozem y características que reflejan un paleoclima seco y de tipo continental. La cima de la secuencia está cubierta por till depositado durante el avance glacial de la etapa Solferino.

Palabras clave: paleosuelo, loess, minerales arcillosos, Chernozem, paleoclima, Pleistoceno superior, Val Sorda, Italia.

INTRODUCTION

Loess deposits are widespread on the Pleistocene terraces contouring the Po Valley fringes (Figure 1) (Accorsi *et al.*, 1990; Chiesa *et al.*, 1990). The loess in northern Italy has been subdivided according to main areas of deposition. On fluvial terraces, loess is found all along the Apennine fringe, from the Piemonte to the Marche region. The thickness of loess deposits increases from northwest to southeast, and thick polygenetic soils have formed in it. On pediments and erosion surfaces, loess has been identified in the Apennine range, between the provinces of Liguria and Marche. At the southern margin of the Prealps, from the Piemonte province to the Tagliamento River, loess deposits are recognized on fluvioglacial terraces and moraine ridges belonging to the glacial stages older than isotope stage 2. At the foothill of the Alps, loess deposits contour upper Pleistocene moraine systems. In the pre-alpine region, loess is widely distributed on the surfaces of periglacial areas, like karstic plateaus (Cremaschi, 1987a). Eolian dusts occur both in caves and rockshelter sediments, in particular on the Lessini Plateau (Cremaschi, 1990b).

The loess is primarily silty in texture, but includes a small amount of sand (1–5%) and the clay content varies between 5 and 40%, depending on the degree of weathering and colluviation processes (Cremaschi, 1990b). Mineralogically, the loess of the Po Plain is rather homogeneous. The fine sand fraction is mainly composed by quartz, feldspar and muscovite (Cremaschi, 1990b). In the fine sand fraction, heavy minerals are especially amphiboles, epidotes, disthene and garnets, along with minerals of metamorphic paragenesis.

We investigated the detailed paleoenvironmental record of the upper Pleistocene loess-paleosol sequence preserved at Val Sorda, Italy. Among the loess-paleosol sequences known in northern Italy, the Val Sorda sequence is undoubtedly one of the most important, because the loess is exceptionally thick (about 5 m) and well preserved. The profile has been the subject of previous studies (Nicolis, 1899; Venzo, 1957, 1961; Mancini, 1960; Fraenzle, 1965; Cremaschi, 1987b, 1990a). Using a methodology similar to Cremaschi (1987b, 1990b) and Accorsi *et al.* (1990), in this research we integrated detailed micromorphology, along with heavy minerals, clay mineralogy, and magnetic parameters with the goal of inferring information about regional weathering processes and paleoclimate. A more general aim of the work is to compare the Val Sorda profile with other upper Pleistocene records from the northern Alpine foreland.

STUDY AREA

The Val Sorda profile is an exposure located on the southeastern margin of Lake Garda (Figure 1), near to the locality of Incaffi (town of Affi). The geographic coordinates
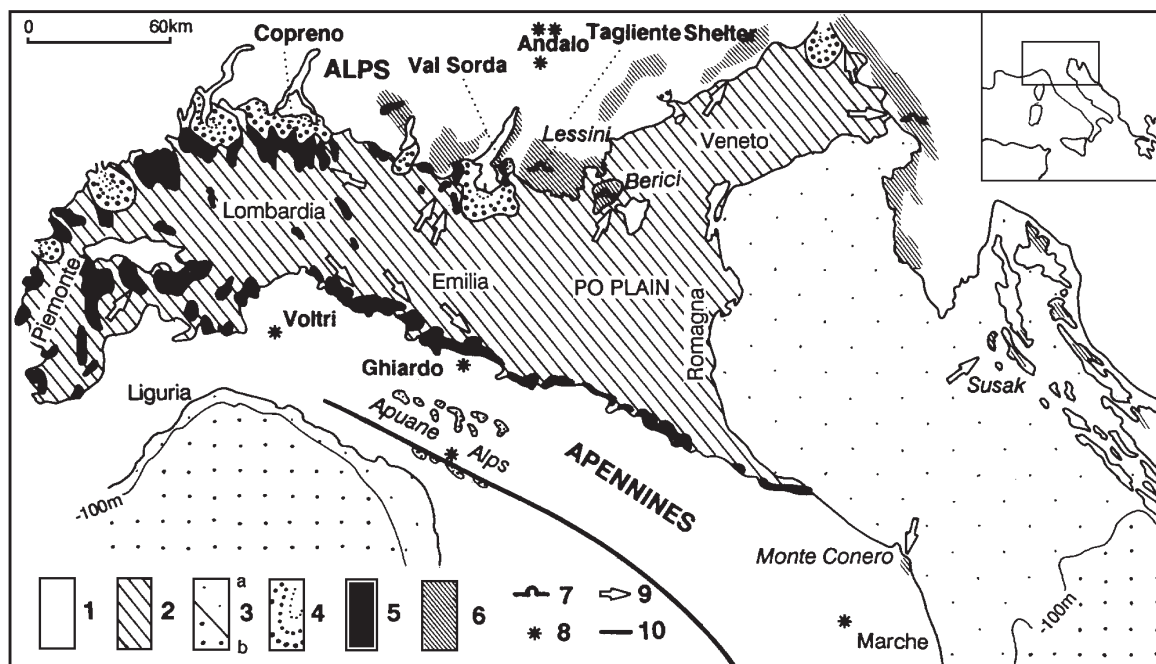

Figure 1. Loess distribution in northern Italy (modified from Cremaschi, 1990a). The geographic position of the Val Sorda profile is indicated. 1: Pre-Quaternary rocks; 2: Late Pleistocene and Holocene alluvial plain; 3: present day sea extent, a: less than 100 m deep, b: more than 100 m deep; 4: Pre-Alpine and Apennine moraine systems; 5: loess deposits on fluvial terraces, fluvioglacial terraces, and moraine ridges; 6: loess deposits on karstic plateaus; 7: loess in caves or shelters; 8: loess on erosional surfaces; 9: direction of dominant winds during loess sedimentation; 10: possible southwest boundary of loess sedimentation during Late Pleistocene.

of the profile are: N 45° 32' 58.3", E 10° 45' 19.4". The 10 m thick profile is situated in the southern slope of the Val Sorda valley at about 220 m a.s.l. and on Mt. Moscal (peak elevation 427 m a.s.l., formed by Miocene calcarenite and Oligocene limestone). During Pleistocene, the Garda glacier reached Mt. Moscal several times, but it was never completely covered (Figure 2). The Val Sorda River originates on Mt. Moscal and flows westwards, towards Lake Garda, near the town of Bardolino. The southwest slope of Mt. Moscal is gently inclined and its lower part has been covered by till and fluvioglacial sediments. The upper part of the slope is covered by loess and the studied sequence is capped by a till deposit. At present, the Val Sorda River is deeply incised into the Quaternary deposits, creating thick exposures on the valleys slopes.

The glacial sediments of the study area belong to the Rivoli Veronese moraine system of the upper Pleistocene Adige glacier. This moraine system has a regular and semicircular shape, made of several concentric arcs (Cremaschi, 1987b, 1990a). The Val Sorda section is covered by some meters of till containing gravel and boulders of limestone, volcanic (porphyries), metamorphic, and intrusive rocks; the matrix is sandy and the deposit is matrix supported, with sand content increasing at the base.

METHODS

Six stratigraphic units are recognized in the exposure and were sampled for laboratory analysis. For field description of the units we used the methods and terminology of Hodgson (1976). In the laboratory, samples were air dried and 2 mm sieved (Gale and Hoare, 1991). About 100 g of the material <2 mm was wet sieved, using 10 sieves (diameter from 1,400 to 63 μm). The composition of the fine fraction (<63 μm) was determined by the sedimentation method using a hydrometer. Heavy minerals were separated from the fine sand fraction (63 μm – 125 μm) (Parfenoff *et al.*, 1970; Mange and Maurer, 1992) using a natrium meta-wolframate [$Na_6O_{39}W_{12}$ (H_2O)] solution (2.9 g/cm^3 density)

and were mounted on glass slides for optical determination. Mineral species were determined with the aid of handbooks and atlases (*e.g.,* Parfenoff *et al.*, 1970; Mange and Maurer, 1992). Undisturbed and oriented soils blocks were collected and thin sections were prepared by the Laboratorio per la Geologia–Piombino, Livorno, Italy. Thin sections were described using the terminology of Bullock *et al.* (1985), with the aid of the interpretative keys (Stoops, 1998). Bulk and clay mineralogy were studied by means of X-ray diffraction (XRD) using the methods described in Terhorst and Ottner (2003). Clay minerals were identified using keys in Brindley and Brown (1980) and Moore and Reynolds (1997). Magnetic properties were analyzed using 10 cm^3 samples collected in cylindrical plastic boxes, with a diameter and height of 25 mm. The following magnetic parameters were measured, according to Walden *et al.* (1999):

1) Magnetic susceptibility (χ). Values were normalized to mass and expressed as mass specific magnetic susceptibility (χ:10^{-8}A m^2/kg);

2) Frequency dependent susceptibility (χ_{fd}). Samples were measured at low frequency (κ_{LF}) (0.465 kHz) and high frequency (κ_{HF}) (4.65 kHz) susceptibility, with values expressed as percentage of frequency dependent susceptibility ($\chi_{fd\%}$);

3) Susceptibility of anhysteretic remanence magnetization (ARM or χ_{arm}).

RESULTS

Field description

The starting point of the description was located at the base of the till deposit covering the loess sequence, about 3 m below the topographic surface. The upper part of the sequence was not described because of thick vegetation cover. The following units were recognized and described from top to bottom (Figure 3):
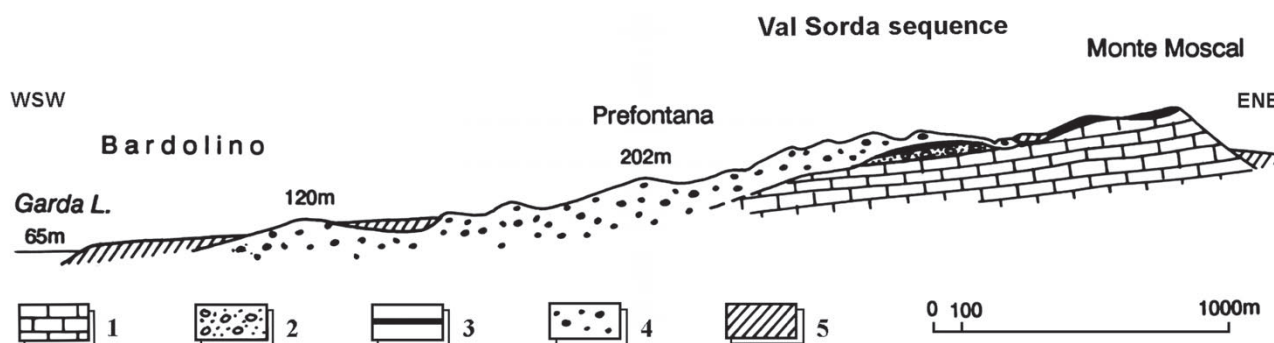
VS1: Till, not described.

Figure 2. Geological section across the Garda moraines and Mt. Moscal. 1: bedrock; 2: till and fluvioglacial deposits (late middle Pleistocene); 3: loess (upper Pleistocene); 4: moraine ridges (late Pleistocene); 5: fluvial deposits (Holocene) (modified from Accorsi *et al.,* 1990).

VS2: Reworked loess changing to laminated glacial sediments (layers from 0–109 cm), containing a white colored zone, very compact (VS 105–109).

VS3: Loess and paleosols unit (VS 109–524 cm); the three buried paleosols have Chernozem morphology developed in loess. The uppermost paleosol (VS 109–350 cm), is well expressed, whereas the properties of the underlying paleosols (VS 350–460 cm and VS 460–524 cm) have weaker morphological expression.

VS4: Reworked colluvial unit. Clayey-sandy level (VS 524–550 cm) containing weathered pebbles and a stone line at the top, which indicate reworking and mixing processes that involve materials both from the overlying and underlying horizons.

VS5: Rubefied paleosol (VS 550–590 cm), dark red in color, with abundant clay, strongly developed angular aggregation, and containing strongly weathered pebbles.

VS6: Glacial and fluvioglacial deposits (>590 cm), in which the rubefied paleosol is developed.

Particle-size analysis

Particle size results are summarized in Figures 4 and 5. Stones are very scarce to absent in the central part of the profile, but there are two areas with increased stone content. One is the uppermost part (VS2/0–70 cm), where colluvial and laminated glacial units are present. The second area is the lower till deposit and the associated paleosol (units VS5 and VS6).

Sand ranges from 9.3 to 31.4 % in all horizons; the average value is 15.5%. Sand percentages are greatest in the laminated glacial (32.8 % in VS2/0–18 cm; Table 1) and colluvial units (from VS2/0–60 cm) as well as in the lower till and the interglacial paleosol (VS5/550–570 cm and VS5/570–590 cm). In most horizons, silt is the dominant fraction, ranging from 30 to 90.7 % (average value 75.9 %). The silt fraction in the Chernozem paleosols shows rather constant distribution (from VS3/109–510 cm) with values ranging from 80.4 to 90.7 %. In the upper part of the profile (VS2/51–60 cm), the silt content is generally reduced, in comparison to the loess deposit, except for the unit we interpret as reworked loess (VS2/18–51 cm). Throughout all horizons, the clay fraction is very low (<10 %) until 510 cm of depth. Only in the Bt-horizon (VS5/550–590) is the clay content enhanced, with values of 25.8% in the upper part and 55.3% in the lower horizon.

Observing the trends shown in Figure 4, it is possible to use particle size data to subdivide the whole sequence in units that are similar to the morphological units, but which illustrate gradation or mixing processes during sedimentation. In Figure 5, selected significant cumulative grain size curves are shown. Curve 1 represents colluviated loess (VS2/51–60 cm), where the stone fraction is 10.3%, sand and silt fractions are present in rather equal amounts (around 30%) and clay is absent. Curve 2 represents the

characteristics of loess (VS3/210–280 cm), where the main component is silt (>80%), whereas sand (10%) and clay (5.1%) occur in lesser amounts. Curve 3 illustrates a Chernozem paleosol (VS3/350–387 cm). The textural characteristics are similar to curve 2. Curve 4 represents the interglacial paleosol (lower part of VS5). The textural characteristics differ from the other samples, because the clay content is strongly enhanced (~47 % average).
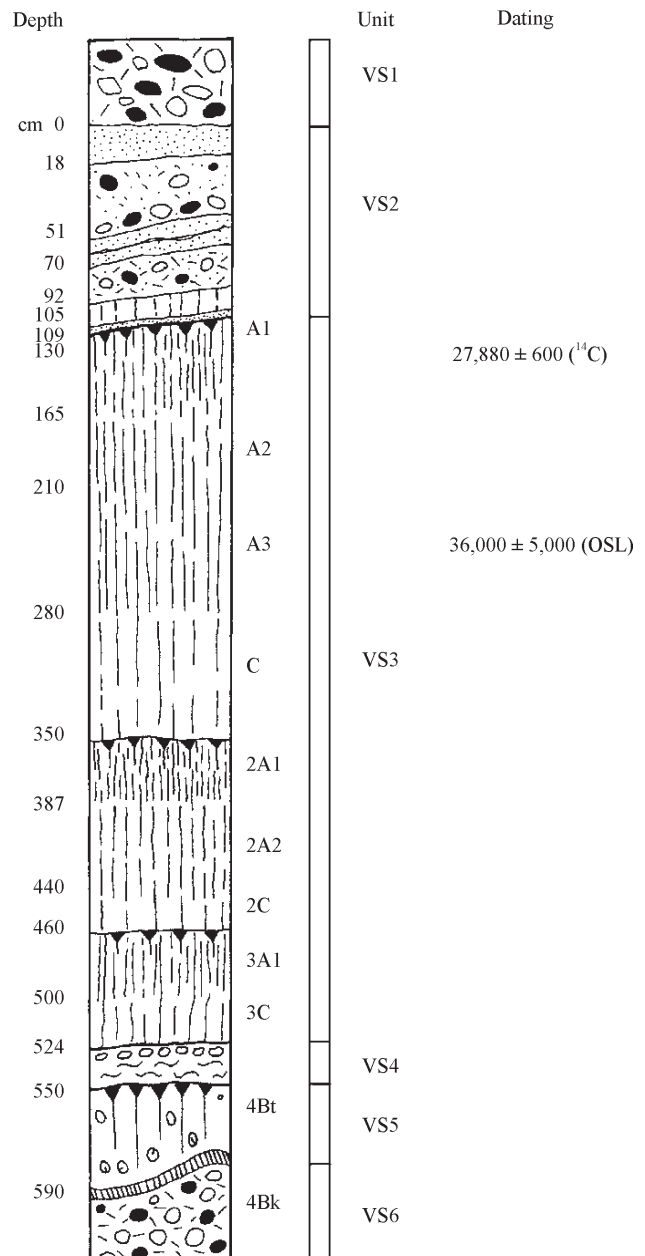

Figure 3. The stratigraphic sequence of the Val Sorda profile. Units and provided in former publications are indicated. Datings (in yr BP) from Cremaschi *et al.* (1987) and Accorsi *et al.* (1990); OSL: Optical Stimulated Luminescence.
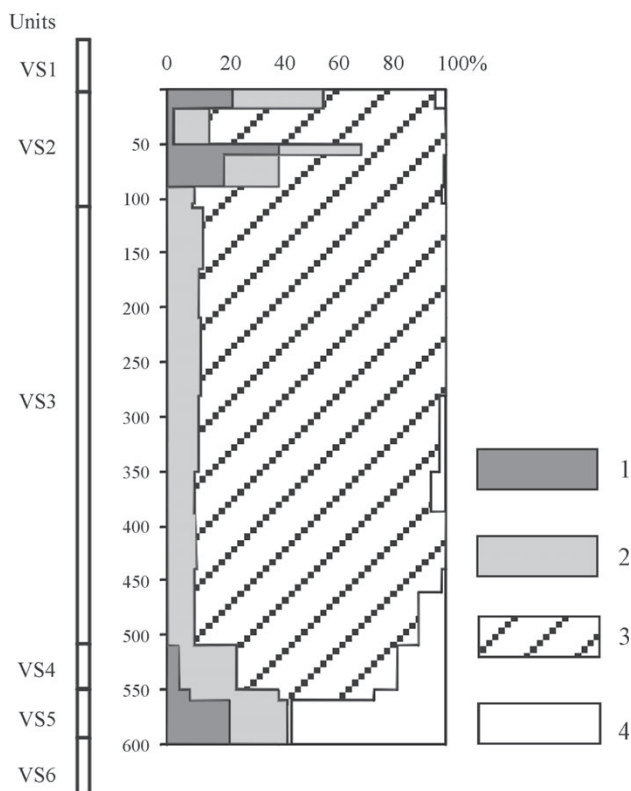
Figure 4. Grain size distribution of the Val Sorda profile, in relation to depth. 1: Gravel; 2: sand; 3: silt; 4: clay.

Heavy minerals

The transparent species range between 83.8 and 91.5% of the heavy fraction (Table 2; Figure 6), being strongly dominant in comparison to opaque minerals. Among transparent minerals, amphiboles are prevalent with an average content of 43.8%; green amphiboles (average content: 36.8 %) and garnets (average content: 23.8%) are abundant. Ultrastable minerals, such as zircon, tourmaline and titanium oxides (only in the form of anatase) are represented only in low percentages and are constant throughout the stratigraphic sequence. Within the profile, only slight differences in heavy mineral composition are observed. Altogether, the composition suggests a metamorphic origin. This supports the proposed Garda system fluvioglacial source of the loess (Cremaschi, 1990b). The homogeneity in the composition of heavy minerals in the loess indicates the same provenance for all.

The profile can be further subdivided on the basis of the heavy mineral composition showed in Figure 6. In VS2, reworked loess and glacial sediments unit, amphiboles are more frequent than epidotes and garnets. In the upper part of unit VS3 (105–210 cm), epidote content increases, which we interpret to reflect a change from glacial to eolian sedimentation. From VS3/210–387 cm (central part of VS3) the percentage of amphiboles decreases by about 10%, while

garnet content show a significant increase. This result corresponds to the thickest part of the loess unit, where the change in heavy mineral composition may indicate the main loess accumulation phase. From VS3/387–524 cm to VS4/550–570 cm (lower part of unit VS3 and VS4), amphibole content increases whereas garnet content decreases. This detailed examination shows that amphiboles are predominant in sediments originating from glacial processes, whereas eolian sediments show an enhanced garnet and epidote spectrum.

Micromorphology

Micromorphological characteristics in thin sections are summarized in Table 3. Porosity is generally low and not well differentiated; voids are mainly channels and planes. The microstructure is apedal throughout the section, except for a (sub)angular microstructure in the paleosols (Figure 7d). C/f related distribution ranges from close to open space porphyric, except for the lower till, where gefuric C/f related distribution occurs.

Throughout the profile, coarse mineral material is mainly composed of subangular quartz and feldspars (coarse silt to fine sand size), common to frequent muscovite flakes (fine sand size), and few (sub)rounded amphiboles (some green) of coarse silt size. Some rounded limestone fragments of the coarse sand size are found in VS2/105–109 cm, while in VS3/135–165 cm these fragments are of gravel size. From VS5/550–590 cm towards the bottom of the profile, rock fragments (limestone and igneous rocks), with pellicular alteration and size ranging from coarse sand to gravel, are common. Their content increases with depth, becoming dominant in the lower till unit.

Fine material, mainly composed of clay, is yellowish-red, or brown with dotted or maculated limpidity. The fine material of the loess portion shows crystallitic b-fabric and in the rubefied paleosol, fine material is darker in color (dark reddish), showing grano/poro striated b-fabric. Organic material consists of some weathered vegetal residues and common fine amorphous organic material. Iron and $CaCO_3$ impregnation is common throughout the profile. Hypocoatings and juxtaposed $CaCO_3$ coatings are common in voids of some layers. These features, in some layers, are composed of euhedral crystals. Frequent fragmented clay coatings exist in VS6/ >590 cm (Figure 7c). Pedorelicts, very strongly iron impregnated, are found in VS3/210–280 and VS3/440–460.

In VS2/105–109 cm we recognized a sedimentary feature consisting of very compact, fine and light material, organized in layers or lenses of different thickness. At the top of this layer and at the boundary of some sub-layers iron intercalations occur. All these features are strongly impregnated with $CaCO_3$. The coarse fraction is composed of quartz and feldspar grains. This zone is very different from the other units because coarse silt and fine sand size
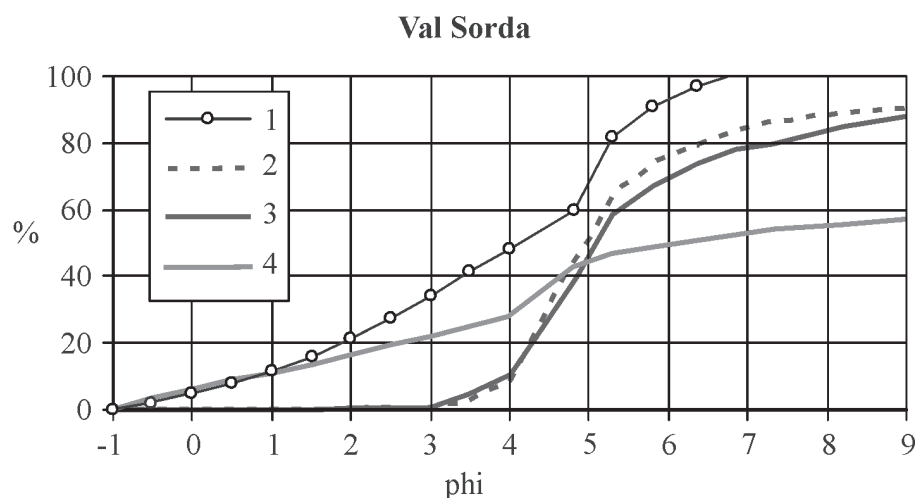
Val Sorda

Figure 5. Some significant cumulative grain size curves from the Val Sorda profile. 1: Colluviated loess, where the sand and silt fractions are present in nearly equal amounts (VS2/51–60 cm); 2: loess curve; main component is silt (>80%), sand and clay are in low percentages (sand ~10%) (VS3/210–280 cm); 3: Chernozem paleosol formed in loess showing textural characteristics similar to curve 2 except for higher clay content (VS3/350–387 cm); 4: curve from an horizon of the rubefied paleosol formed in till; main component is clay (~47%), in consequence of strong pedogenetic activity; sand and silt (respectively ~ 28 and 25%) are also quite common (VS5/570–590 cm).

fractions dominate, organized in compact thin layers or lenses (Figure 7a). The relative lack of fine material and the sedimentological fabric could be the consequence of subglacial phenomena: melt water washed the fine fraction away and the load pressure exerted by the overlying glacier compacted the material.

The micromorphological analysis confirms most of the field observations: the main component of these deposits is loess sediment composed of angular to subangular quartz and feldspars, and silt-sized muscovite flakes (Figure 7b). In addition, it is characterized by apedal microstructures (except for VS2/105–109 cm), with low porosity, which indicates the influence of pressure from the glacier. Many samples, also coming from the loess unit (VS3), contain rounded rock fragments and/or pedorelicts; their abundance suggests the intensity of reworking and colluvial processes. Voids are rounded channels (associated with biological activity), often totally or partially filled with $CaCO_3$, and vugs. Organic material is composed of amorphous fine material and, locally, strongly weathered plant remains. We observed organic matter distributed over a considerable depth, indicating a continuous pedogenetic process, although probably slowed by the new eolian inputs.

Pedological features are not well differentiated. $CaCO_3$ features are the most common; in particular, coatings and hypocoatings in bioturbation channels suggest secondary precipitation. In the groundmass, iron accumulation is common, but only moderately impregnated. The rubefied paleosol is characterized by common thick fragmented clay coatings, iron impregnation in the groundmass, and manganese impregnation and small nodules. We interpret all these evidences as indicative of strong weathering and illuviation processes.

Mineralogy

Bulk mineralogy

VS1, parts of VS2 and VS6. The upper and the lower till as well as the thin white layer (VS2/105–109 cm) consist mainly of calcite and dolomite. Additionally, small amounts of quartz, plagioclase, and traces of layer silicates and

Table 1. Percentage abundance of every sampled unit of the Val Sorda profile.

Unit	Stones	Sand	Silt	Clay
VS 0–18	23.2	32.8	40.1	3.9
VS 18–51	2.5	12.4	85.1	0.0
VS 51–70	40.1	29.9	30.0	0.0
VS 90–105	0.0	10.0	88.8	1.2
VS 105–109	0.0	9.3	90.7	0.0
VS 109–130	0.0	13.0	87.0	0.0
VS 130–165	0.0	11.0	89.0	0.0
VS 165–210	0.0	12.3	87.7	0.0
VS 210–280	0.0	10.0	84.9	5.1
VS 350–387	0.0	10.0	89.0	1.0
VS 387–440	0.0	10.5	89.5	0.0
VS 440–460	0.0	10.0	88.1	1.9
VS 460–510	0.0	10.0	80.4	9.6
VS 550–570	8.6	31.4	34.2	25.8
VS570–590	22.6	20.3	1.7	55.3

Table 2. Heavy minerals assemblage of the profile (expressed in %).

| VS	0 – 18	18 – 51	51 – 70	90 – 105	105 – 109	109 – 130	130 – 165	165 – 210	210 – 280	350 – 387	387 – 440	440 – 460	460 – 510	550 – 570	570 – 590
Transparent	89.82	87.22	89.60	88.07	90.34	85.88	88.96	89.12	89.07	86.52	83.80	91.52	89.07	87.88	91.48
Opaque	10.18	12.78	10.40	11.93	9.66	14.12	11.04	10.88	10.93	13.48	16.20	8.48	10.93	12.12	8.52
Zircon	1.33	1.91	0.65	0.65	1.89	1.32	0.73	0.58	0.00	0.00	0.67	0.66	1.23	2.76	1.86
Tourmaline	0.67	1.91	0.00	3.23	0.00	3.29	0.73	4.07	2.45	1.30	1.33	1.99	1.84	0.69	1.24
Rutile	0.67	0.64	0.65	0.65	1.26	0.66	0.00	0.00	1.23	1.30	2.00	1.32	1.23	0.00	0.00
Brookite	0.00	0.00	0.00	0.00	0.00	0.00	0.00	0.00	0.00	0.00	0.00	0.00	0.00	0.00	0.00
Anatase	0.67	0.64	0.65	0.00	0.00	0.00	0.00	0.00	0.00	0.00	0.00	0.00	0.00	0.00	0.00
Green Amphibole	48.67	41.40	43.87	29.03	28.30	33.55	37.96	36.63	30.06	23.38	34.67	40.40	28.83	40.69	54.66
Brown Amphibole	7.33	5.10	11.61	4.52	5.03	5.92	4.38	2.33	3.07	1.95	1.33	3.31	3.68	4.83	0.62
Other Amphibole	1.33	1.91	3.87	0.65	5.03	1.97	0.00	2.91	1.84	3.25	4.00	2.65	5.52	3.45	2.48
Pyroxene	14.00	10.19	9.03	12.26	16.98	8.55	9.49	11.63	7.98	14.94	8.00	9.93	14.11	6.90	8.70
Epidote	0.67	1.91	3.23	7.74	11.32	5.92	14.60	12.79	11.66	11.04	12.00	4.64	10.43	13.10	16.15
Garnet	20.00	22.29	17.42	30.97	22.64	28.95	24.82	22.67	34.97	38.31	26.67	25.83	26.38	7.59	8.70
Baryte	0.00	0.00	0.00	0.00	0.00	0.00	1.46	0.00	0.00	0.00	5.33	2.65	2.45	0.00	0.00
Kyanite	0.00	0.00	0.00	0.00	0.00	0.00	0.00	0.00	0.00	0.00	0.00	0.00	0.00	0.00	0.00
Sillimanite	0.00	0.00	0.00	0.00	0.00	0.00	0.00	0.00	0.00	0.00	0.00	0.00	0.00	0.00	0.00
Corundum	0.00	0.00	0.00	0.00	0.00	0.00	0.00	0.00	0.00	0.00	0.00	0.00	0.00	0.00	0.00
Andalusite	0.00	0.00	0.00	0.00	0.00	0.00	0.00	0.00	0.00	0.00	0.00	0.00	0.00	0.00	0.00
Sphene	0.00	0.00	0.00	0.00	2.52	1.32	0.00	2.33	2.45	0.65	0.67	0.00	0.00	1.38	0.00
Spinel	0.00	0.00	0.00	0.00	0.00	0.00	0.00	0.00	0.00	0.00	0.00	0.00	0.00	0.00	0.00
Allanite	0.00	0.00	0.00	0.00	0.00	0.00	0.00	0.00	0.00	0.00	0.00	0.00	0.00	0.00	0.00
Staurolite	1.33	1.91	1.94	1.29	0.00	0.66	0.73	0.00	0.00	1.95	0.00	0.66	0.00	0.69	0.00
Altered	3.33	10.19	7.10	9.03	5.03	7.89	5.11	4.07	4.29	1.95	3.33	5.96	4.29	17.93	5.59
Whr	0.03	0.07	0.01	0.08	0.03	0.09	0.03	0.09	0.06	0.03	0.04	0.05	0.06	0.06	0.05
Alteration index	0.05	0.08	0.03	0.08	0.05	0.09	0.02	0.07	0.07	0.05	0.07	0.07	0.07	0.05	0.04
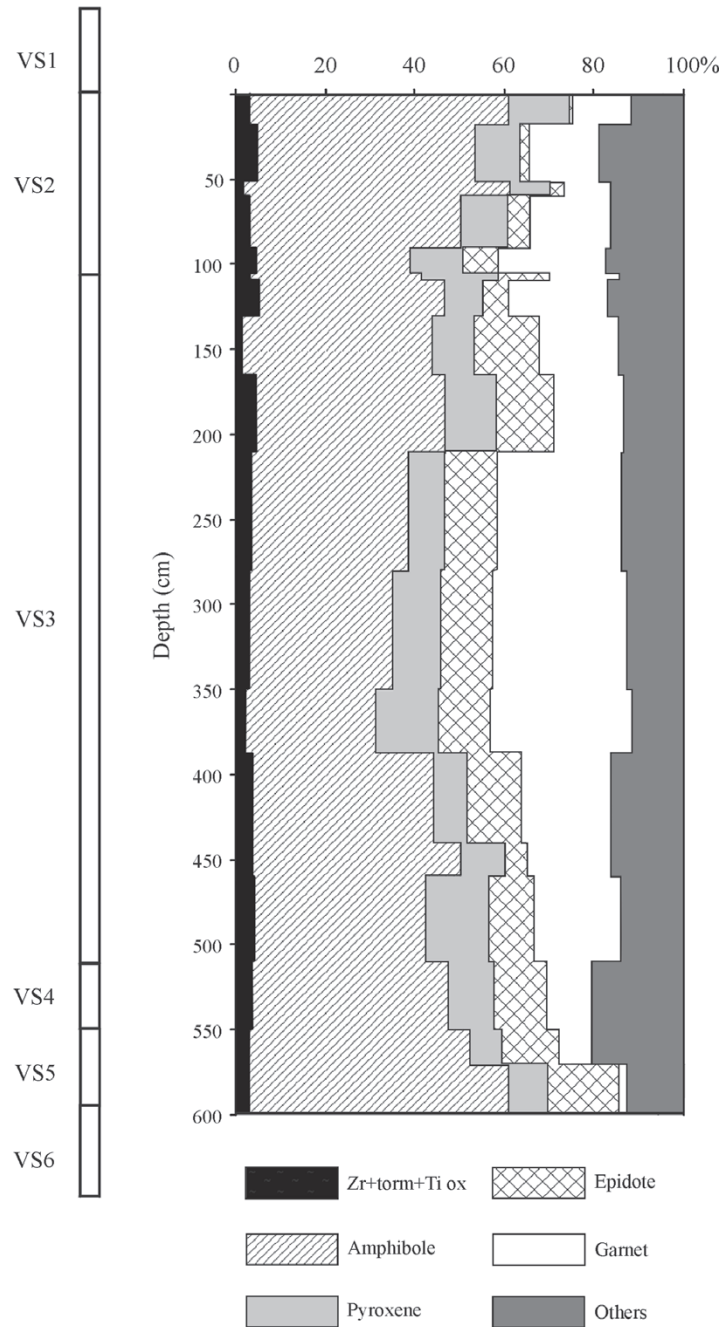
Figure 6. Depth trends of heavy minerals at Val Sorda.

amphiboles occur. The presence of these minerals and the absence of K-feldspar indicate a source area consisting mainly of carbonate rocks.

VS3. In contrast to the till samples, carbonate minerals occur in small amounts in the loess samples and the vast majority of the loess is free of carbonate. Significantly higher amounts of plagioclase and muscovite are present in the upper part of the loess sequence compared to the lower part.

Quartz occurs in moderate amounts in all loess samples, and shows no obvious trend within the sequence. Amphiboles are detectable in small amounts within the whole sequence, but somewhat higher values are found in the upper part. The three weakly developed paleosol horizons could not be distinguished by differences in the bulk mineral composition.

VS5. The rubefied paleosol not only differs

Table 3. Summary table of micromorphological characteristic of the profile.

Voids	Microstructure	C/f (limit; ratio; rel. distribution)	Coarse material	Fine material	Organic material	Pedofeatures
VS 105-109						
Porosity is few and not well differentiated: few rounded channels(f sa); very few elongated chambers (f sa); few vughs (m - f sa)	Pedal; channel microstructure	20 µm; 4/1; close porphyric	Dominant subangular quartz and feldspars (c si - f sa); very frequent muscovite flakes (fi sa); few rounded amphiboles (some green) (c si); very few rounded limestone fragments (c sa - g)	Yellowish, dotted limpidity, crystallitic b-fabric	Very few vegetal residues, with iron coating	Sedimentary feature, consisting of very compact fine and light material, organised in layers or lenses of different thickness. Iron intercalations, moderately impregnated are at the top of this layer (thickness of the fine sand) and at the boundary of some sub-layers (thickness of the coarse silt); all this feature in strongly CaCO₃ impregnated; the coarse fraction is made of quartz and feldspars grains (coarse fraction)
VS 109-130						
Porosity is few and not well differentiated and less than the above level; very few rounded channels (f sa)	Apedal; massive microstructure	20 µm; 9/1; close porphyric	Dominant angular quartz and feldspars (m si - f sa); common muscovite flakes (m si - f sa); few subrounded amphiboles (some green) (c si)	Reddish, dotted limpidity	Very few vegetal residues, strongly weathered; common fine amorphous organic material	Iron impregnations, moderately impregnated, are common, dispersed in the ground mass
VS 109-130-soil						
Very few planes, partially accommodated (f sa); few rounded channels (f sa)	Apedal; channel microstructure	20 µm; 4/1; close porphyric	Dominant angular to subangular quartz and feldspars (m - c si); very frequent muscovite flakes (f sa); few subangular to subrounded amphiboles (some green) (f sa)	Yellowish-red, crystallitic b-fabric	Very few weathered vegetal residues	Iron impregnations, moderately impregnated, are very common; iron intercalations (height of the fine sand), in shape of diagonals lines in the section; pedorelict of centimetric size very red in colour; his ground mass is strongly CaCO₃ impregnated and the coarse fraction is similar to the one described for the section
VS 130-65						
Few rounded channels (f sa)	apedal; channel microstructure	20 µm; 4/1; close porphyric	Dominant subangular quartz and feldspars (coarse si); frequent muscovite flakes (length: f sa); very few subangular to subrounded amphiboles (some green) (f sa); rare rounded limestone fragments (f sa)	Reddish, dotted to cloudy limpidity	Common amorphous organic material	Iron impregnations, moderately impregnated, are common; frequent iron intercalations, strongly impregnated
VS 165-210						
Rare rounded channels (f sa); few vughs (f sa)	Apedal; vughy microstructure, very weakly developed	10 µm; 7/3; close porphyric	Dominant angular to subangular quartz and feldspars (f sa); frequent muscovite flakes (length: f sa); few subrounded amphiboles (some green) (c si)	Yellowish-brown, cloudy limpidity	Few amorphous organic material	Common iron intercalations (fine sand size), moderately impregnated, in the shape of oblique lines that cross the section; common iron rounded nodules weakly impregnated, with not marked boundaries; frequent CaCO₃ impregnations; CaCO₃ hypocoatings and juxtaposed coatings in some voids (height of the fine sand); the CaCO₃ features are slightly iron impregnated
VS 210-280						
Few rounded channels (c si); few rounded vughs (f sa)	Apedal; vughy microstructure, very weakly developed	10 µm; 7/3; close porphyric	Dominant angular to subangular quartz and feldspars (c si - f sa); frequent muscovite flakes (length: f sa); rare subrounded amphiboles (some green) (f sa)	Reddish-brown, cloudy limpidity	Common amorphous organic material; few very weathered plant remains	Common iron intercalations (fine sand size), strongly impregnated; CaCO₃ slightly iron impregnated, hypocoatings and juxtaposed coatings in some voids, very thick (height of the medium sand), in some voids, the coating is composed of euhedral CaCO₃ crystals; frequent pedorelicts, very strongly iron impregnated

Table 3. Continued.

| Voids	Microstructure	C/f (limit; ratio; rel. distribution)	Coarse material	Fine material	Organic material	Pedofeatures
VS 440-460						
Frequent rounded channels (c si - f sa); frequent vughs, slightly elongated (c sa)	Apedal; vughy microstructure, very weakly developed	10 μm; 4/1; close porphyric	Dominant subangular quartz and feldspars (c si - f si) common muscovite flakes (length: f - m sa); rare subrounded amphiboles (some green) (c si)	Yellowish - red, maculated limpidity	Common amorphous organic material.	Common iron intercalations (fine sand size, strongly impregnated; very frequent pedorelicts, very strongly iron impregnated; one centimetric pedorelict consisting of a CaCO₃ nodule, with few grains and voids inside, with an iron hypocoating around it.
VS 460-500						
Few planes, partially accommodated of the coarse sand size; frequent vughs (f sa)	Apedal; vughy microstructure	20 μm; 4/1; close porphyric	Very common muscovite flakes (length: f - m sa); common subangular quartz and feldspars (c si); few subrounded piroxenes and amphiboles (c sil)	Yellowish - red, maculated limpidity	Common amorphous organic material.	Frequent iron elongated intercalations (medium sand size), moderately, impregnated
VS 524-550						
Common accommodated planes (m sa)	Apedal; fissure microstructure	20 μm; 4/1; close porphyric	Common angular quartz and feldspars (m sa, very common muscovite flakes (length: c si); few subrounded piroxenes and amphiboles (c si)	Yellowish - red, dotted limpidity, granostriated, locally striated b-fabric	Common amorphous organic material.	Common iron hypocoatings (medium sand size), strongly impregnated
VS 550-590						
Common accommodated planes (m sa)	Subangular blocky, well developed microstructure	20 μm; 1/1; open space porphyric	Common subangular quartz and feldspars (f sa); few subrounded piroxenes and amphiboles (c si); common rounded rock fragment (c sa)	Reddish, dotted limpidity, granostriated, b-fabric	Common amorphous organic material.	Common iron nodules (coarse sand size), moderately impregnated.
VS >590						
Frequent accommodated planes (m sa); frequent rounded channels (m sa); common vughs (f sa)	Angular elongated aggregates; vughy microstructure	20 μm; 1/1; open space porphyric	Common subangular quartz and feldspars (m sa - m si); few subrounded piroxenes and amphiboles (c si); common rounded rock fragment (limestone and igneous rocks), with pellicular alteration (c sa)	Reddish, dotted limpidity, granostriated b-fabric	Few vegetal fragments (fine - medium sand size)	Common fragmented yellowish - red clay coatings (medium sand size); common CaCO₃ infillings in pores, moderately iron impregnated
VS-lower till						
Few simple packing voids (f - m sa); frequent, partially accommodated planes (m sa); common rounded channels (f - m sa)	Apedal; channel microstructure	20 μm; ratio 9/1; gefuric	Frequent subangular quartz and feldspars (f - m sa); frequent subrounded calcite (m sa); dominant rounded rock fragment (limestone and igneous rocks), with pellicular and irregular alteration (centimetric size)	Reddish, maculated limpidity	Common vegetal fragments of medium sand size)	Common, locally fragmented, yellowish - red clay coatings (medium sand size); frequent, rounded or elongated, iron nodules, strongly impregnated (fine sand - coarse silt size); common CaCO₃ infillings in pores, moderately iron impregnated
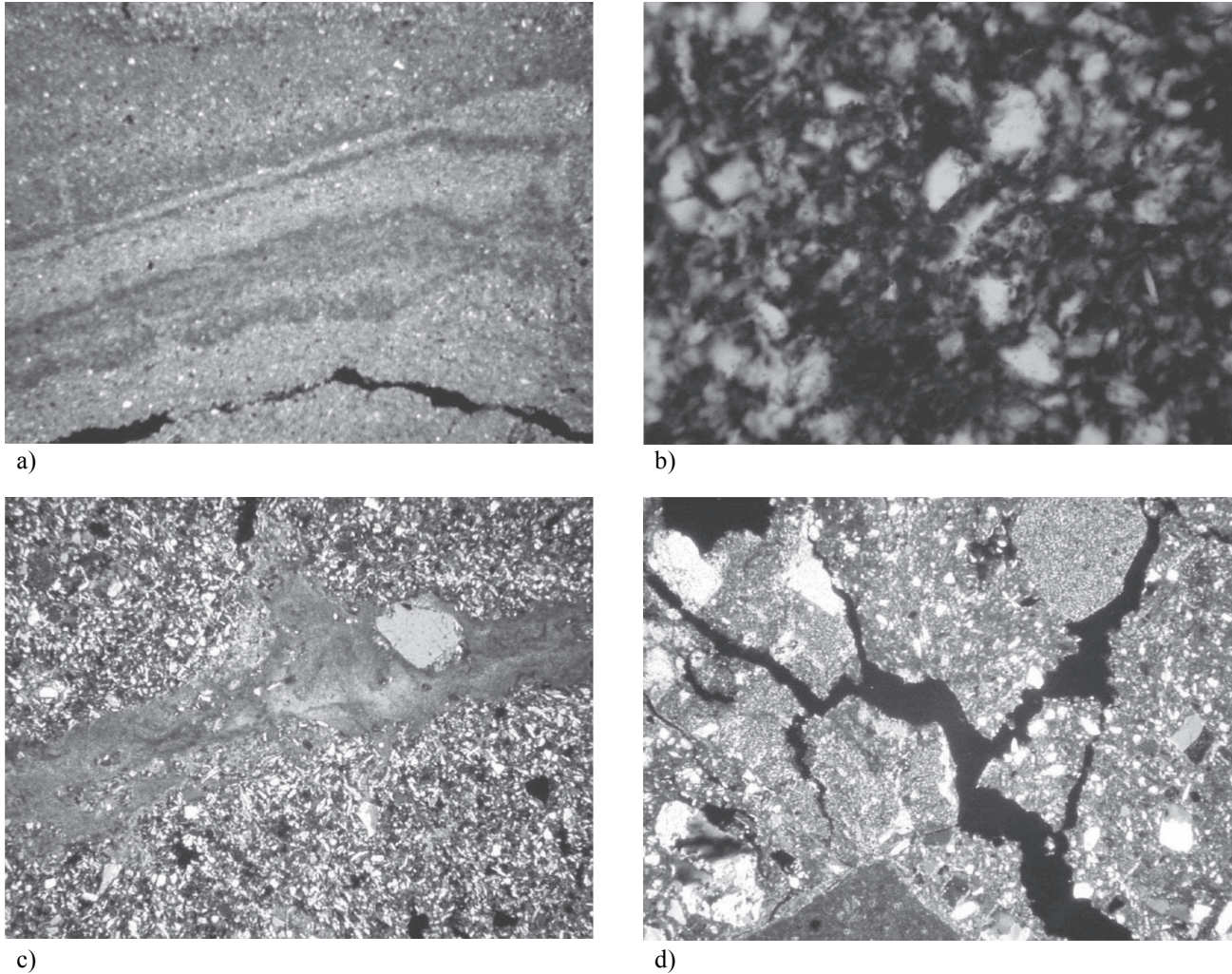
Figure 7. Micromorphological characteristics of some Val Sorda levels. a) Detail of sedimentary feature consisting of layers or lenses of very compact fine and light material, strongly CaCO₃ impregnated (1.6x XPL; VS2/105-109 cm); b) loess deposit in the Chernozem soil, rich in organic matter and containing iron impregnations (10x PPL; VS3/130-165 cm); c) iron-rich clay intercalation in the groundmass of the lower Chernozem soil (1.6x PPL; VS3/460-500 cm); d) subangular polyhedric aggregates of the Eemian paleosol (1.6x XPL; VS5/550-590 cm).

significantly in color from the other units, but also in mineralogy. The dark-red color is due to the presence of hematite. Layer silicates dominate, and all other minerals (*e.g.*, quartz, feldspar) occur in rather small amounts. Carbonate minerals, chlorite, and amphiboles are below the detection limit of the XRD. At the bottom of the paleosol, strongly weathered rocks of different composition occur, such as metamorphites rich in amphiboles, limestone, along with magmatic rocks rich in quartz and feldspars. Most of them are transformed to clay minerals dominated by vermiculite.

Clay mineralogy

For the clay mineralogical analyses, the same samples as for the bulk mineral analyses were used. All values refer to the clay fraction (<2 μm) and are normalized to 100 mass % clay minerals.

VS1 and VS6. The clay fraction (<2 μm) is dominated by illitic material with over 60 mass %, with chlorite, smectite, and kaolinite occurring in minor amounts. Generally, the reflection intensity of the clay minerals is rather weak. The crystallinity of the illite is poor. The smectite appears to be low charged, as there is no contraction of the 14 Å peak to 10 Å after K-saturation and no clear expansion to 17 Å after saturation with ethylene glycol. The main part of the kaolinite is expandable with dimethylsulfoxide (DMSO), indicating that it is well crystallized and not neoformed. Low quantities of chlorite are present both in the upper and in the lower till. The small amounts of this mineral do not allow a fully characterization or quantification. The presence of smectite in the till indicates that older, already weathered sediments and soils could have been incorporated into the glacial material. Even in the clay fraction (<2 μm), high amounts of calcite and
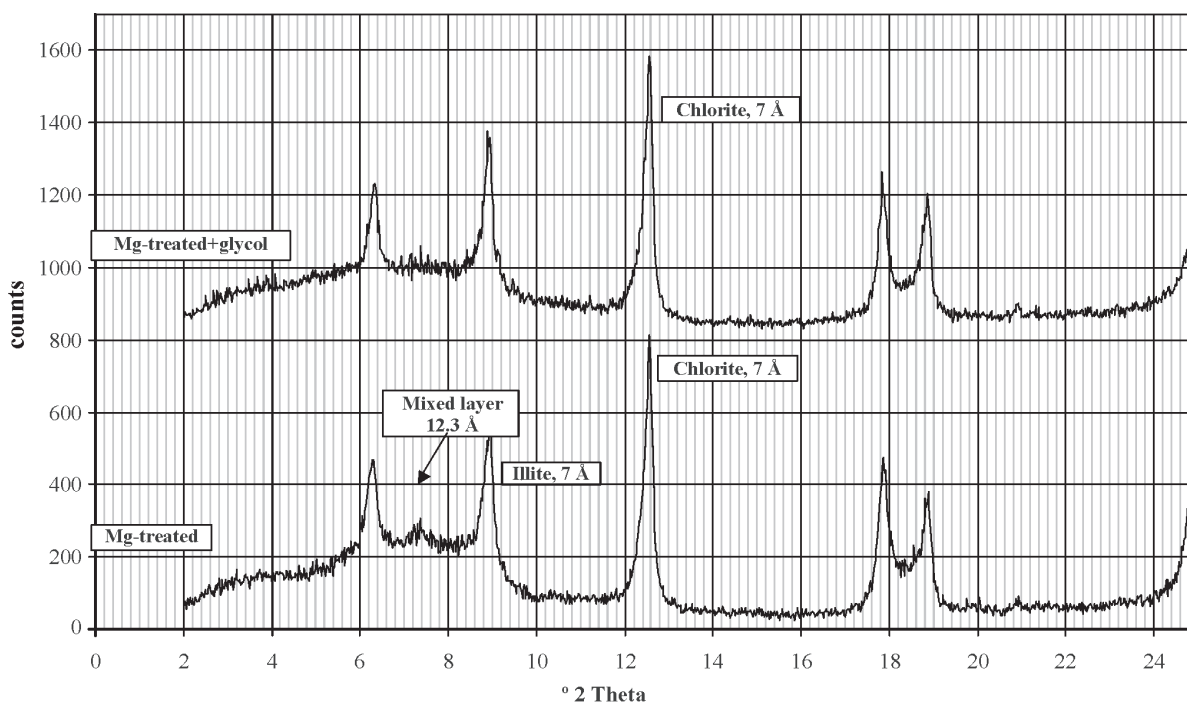
Figure 8. Diffractograms of the clay fraction of a loess sample after treatment with Mg^{2+} and K^+. Reflections of illite, chlorite, and a mixed layer mineral are labeled.

dolomite are present, reflecting the limestone that dominates the source area.

VS2. The clay mineral composition is very similar to that of the till, *i.e.,* more than 60 mass % illite and minor amounts of smectite, kaolinite, and chlorite. High amounts of carbonate minerals are present in the clay fraction as well. The similar clay mineral composition supports our observation regarding a common source for the reworked unit and the overlying till.

VS3. Illite is present between 46 and 70 mass % and is the main clay mineral in all loess samples. Its crystallinity is quite high, indicating weak weathering influence (Figure 8). Primary chlorite is of secondary importance, with 21 to 37 mass %. Kaolinite is detectable in only very small amounts (2–6 mass %), vermiculite (14Å) is detectable only in the uppermost and lowermost loess samples. All samples contain a mixed layer mineral (6–13 mass %), most likely composed of illite and smectite. Smectite is not detectable in the loess samples. After heating to 550°C, the Mg-exchanged samples show a significant increase in peak intensities, indicating some recrystallization must have occurred. Except for the sporadic occurrence of vermiculite, the samples in the whole loess sequence are generally homogeneous. Clay minerals of the three paleosol horizons cannot be distinguished from the loess units they formed in, supporting our morphological interpretation of weak expression and minimal pedogenesis.

VS5. As in the bulk mineralogical composition, the rubefied paleosol shows significant differences in the clay mineralogical association compared to the other parts of the sequence. Primary chlorite is not detectable, which we interpret as a result of weathering during the Eemian interglacial. Illite is still predominant, with values between 42 and 59 mass %, much less than in the loess sequence. Vermiculite (Figure 9) is present up to 48 mass %, and in some samples its content surpass that of illite. Compared to the loess sequence, the chemically stable kaolinite can be found in significantly higher contents. It is poorly crystallized, which means that the kaolinite is pedogenetically formed (Durn *et al.*, 1999). The illite–smectite mixed-layer mineral can also be detected in traces in the rubefied paleosol. Smectite is absent. Very strongly weathered pebbles are abundant in the rubefied paleosol. They are mostly very soft and easily visible in the fine soil because of their different color. They are composed mostly of vermiculite (Figure 10).

Below the rubefied paleosol and in the uppermost part of the till, there is a transitional horizon. This horizon has characteristics of both the above paleosol horizon and the underlying till. It has the same clay mineralogical composition as the till, but the clay fraction is free of carbonates, like in the paleosol.

The differences in the clay mineralogical composition of loess and paleosols are evident when comparing the 060-reflections of the clay fractions. The samples from the loess sequence show two major peaks, one at d=1.535 Å and the
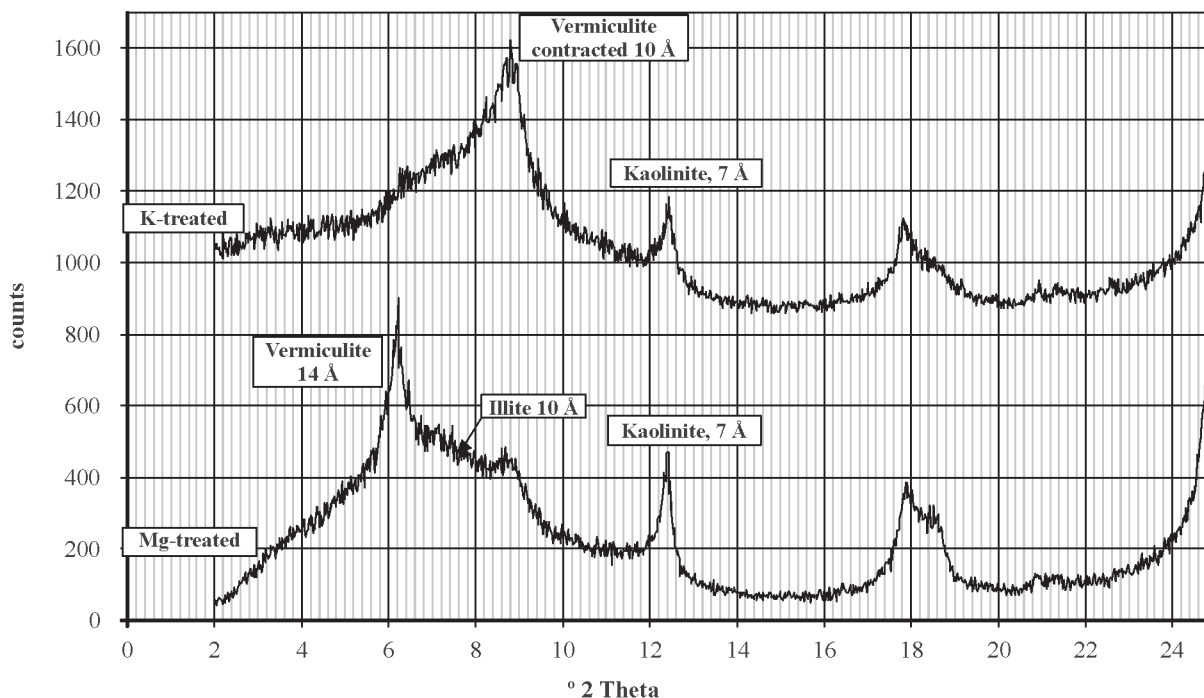
Figure 9. Diffractograms of the clay fraction of the rubefied paleosol. The K$^+$ treatment illustrates the contraction of vermiculite to 10 Å.

other at d=1.50 Å. The 1.535 Å-peak represents trioctahedral clay minerals in the sample, with primary chlorite as the most important mineral of that group. The 1.50 Å-peak represents dioctahedral clay minerals, *e.g.* illite, kaolinite and mixed-layer minerals. In the rubefied paleosol, only one reflection at 1.50 Å is observed, indicating that only dioctahedral clay minerals are present. Therefore, the occurring vermiculite in the paleosol must be dioctahedral.

Magnetic property analysis

The intensity of magnetic susceptibility (MS) of the Val Sorda sequence varies significantly with depth (Figure 11a), with a main trend to increasing concentration of ferrimagnetic minerals with depth. Throughout unit VS2, magnetic susceptibility values are low, gradually increasing with depth, including into the upper portion of VS3. This trend suggests that the glacial sediments incorporated loess at the base. Beginning at 180 cm, the magnetic susceptibility increases in small steps. The first increase occurs in the upper part of the buried Chernozem (VS3/130–210 cm). There is a second, stronger enhancement in unit VS3/210–280 cm, in the lower part of the upper buried Chernozem paleosol. This observation coincides with the occurrence of well developed iron impregnation observed in thin section. The third increase corresponds to the second buried Chernozem (VS3/350–387 cm). From this point on, magnetic susceptibility shows similar values throughout the lower part

of unit VS3. In the basal (third) buried Chernozem (VS3/ 460–524 cm) only a weak increase is recognized. We consider the higher MS values in the paleosols correlated with the increase in the content of ultrafine ferrimagnetic minerals produced *in situ* by weathering and bacterial activity (Maher, 1998).

From a general point of view, the magnetic susceptibility of the whole loess unit VS3 is rather homogeneous, but enhanced in comparison to the magnetic susceptibility of the glacial sediments. The values in the central portion of the loess unit VS3 are slightly enhanced, maybe corresponding to the main loess accumulation phase. Buried Chernozem profiles show only a weak increased rate of concentration of ferromagnetic minerals, with respect to the unweathered loess. This evidence indicates that the magnetic signal for this portion of the profile could be interpreted as a sedimentation signal, more than as a weathering one.

A significant peak occurs in the reworked layer (VS4) and in the Bt-horizon of the interglacial paleosol (VS5). In the interglacial paleosol (VS5), the concentration of ferromagnetic minerals is strongly enhanced as a response to intense pedogenetic processes. First decreasing tendencies but also some strong variations and positive peaks occur in unit VS6, where the glacial and fluvioglacial deposits are present.

Frequency dependent susceptibility ($\chi_{fd\%}$) values (Figure 11b) can give more detailed information about the ultrafine superparamagnetic (SP) ferrimagnetic mineral
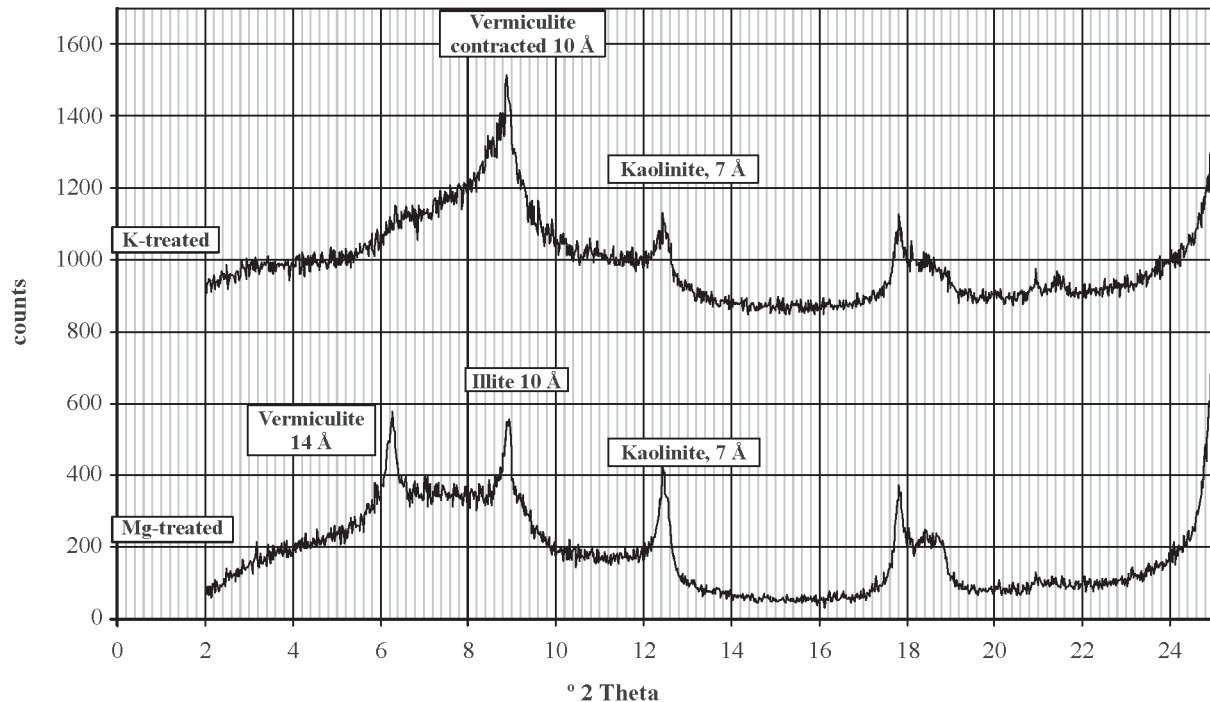
Figure 10. Diffractograms of a strongly weathered pebble in the rubefied paleosol. It consists of high amounts of vermiculite (pay attention to the strong contraction of vermiculite after K-treatment). This result proves that the vermiculite from the pebbles constitute the source of vermiculite in the clay fraction.

grains (particularly magnetite). The main trend observed is a slight increase in $\chi_{fd\%}$ with depth, although values fluctuate. Samples from the upper till deposit (VS1) show very low values, while values are enhanced in the loess deposit (VS3) including two intervals with higher values. The higher values occur in the lower part of the first Chernozem (165–280 cm) and from 350 to 450 cm in the underlying Chernozem paleosol. Values in the third (basal) Chernozem paleosol are reduced. On the contrary, in the reworked layer (VS4) and the rubefied paleosol (550–590 cm and deeper VS6) $\chi_{fd\%}$ values increase significantly, reaching average values of 34.5 %, with a maximum value of 43.9 %. On the basis of these results, it is possible to conclude that ultrafine superparamagnetic ferrimagnetic mineral grains (magnetite) are detected throughout the sequence. Maximum values are observed in the two upper Chernozem paleosol profiles and, in particular, in the rubefied paleosol and its overlying colluvial layer, indicating predominance of pedogenic control in the distribution of ultrafine magnetic minerals.

The ARM analysis results (Figure 11c) are characterized by a very clear trend. In the upper till (VS1), values are close to zero; from this point on, values generally increase with depth. Throughout unit VS3, values increase stepwise; the first increase occurs between VS3/130–210 cm in the upper buried Chernozem. The lower horizon of the Chernozem shows enhanced values and they reach a maximum in unit VS3 (at 210–280 cm) in the lower part of the upper buried Chernozem. A marked peak occurs in the

second buried Chernozem (350–440 cm), whereas the third buried Chernozem is characterized by slightly lower values. Figure 11c shows the maximum values in the reworked layer (VS4) and the underlying interglacial paleosol (VS5), while the lower till (VS6) is characterized by rather low values.

The content of stable single domain (SSD) ferrimagnetic grains in the Val Sorda profile is enhanced in the lower part of the upper buried Chernozem (the SP ferrimagnetic grains show the same trend). The second peak can be seen in the second buried Chernozem (both for fine and ultrafine ferrimagnetic grains). The lower basal buried Chernozem neither contains many ferrimagnetic minerals, nor ultrafine or fine grains. Comparing the reworked layer (VS4) with the underlying paleosol (VS5), it becomes clear that the colluvial layer contains more SSD ferrimagnetic minerals and less SP ferrimagnetic minerals than the paleosol. A possible explanation is that magnetic minerals from the reworked layer (VS4) are derived from reworking of the upper and more weathered horizons of the rubefied paleosol. These observations allow to conclude, that ferrimagnetic minerals present in these two units are different from each other: the colluvial layer consists of ferrimagnetic minerals especially in the SSD (fine) form; the interglacial paleosol contains more ferrimagnetic minerals of the ultrafine dimension (SPD), due to strong pedogenesis. As the colluvial layer is a mixture of soil material and unweathered sediments it consists of less SPD minerals and more SSD minerals.
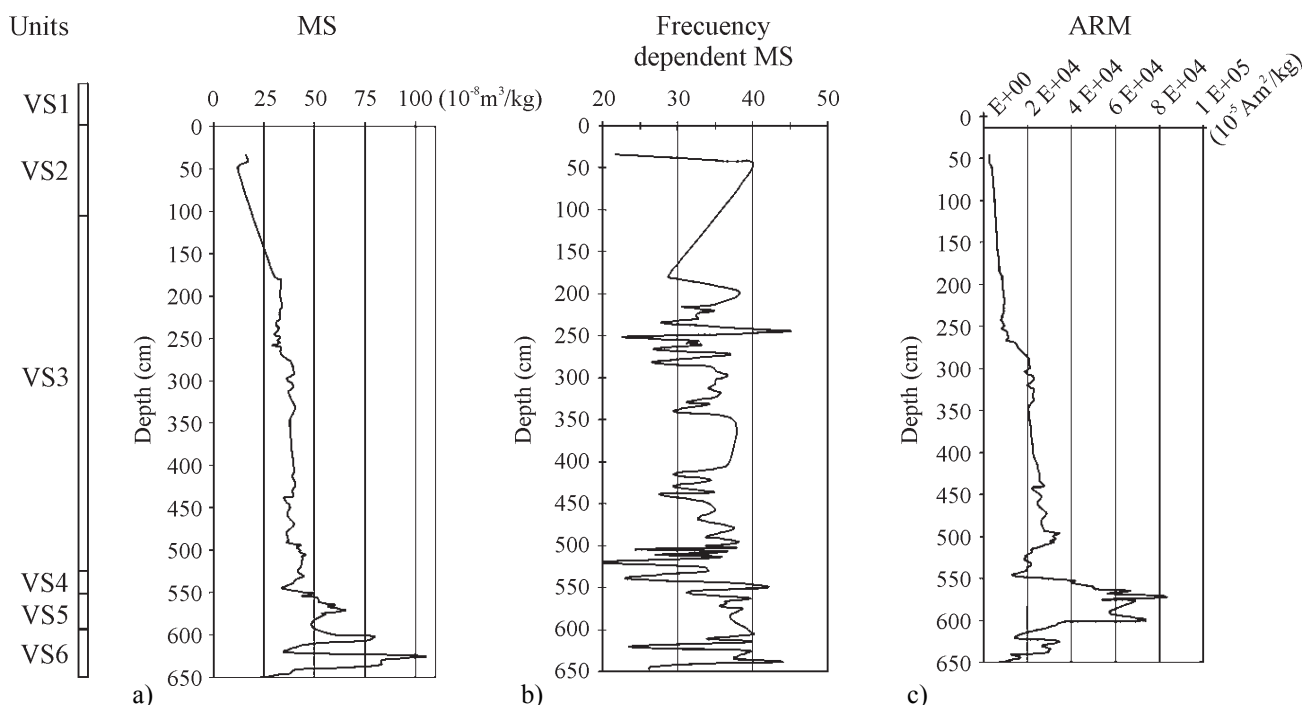
Figure 11. Magnetic susceptibility results from the Val Sorda profile. a) Mass specific magnetic susceptibility; b) frequency dependent susceptibility; and c) anhysteretic remanence magnetization.

DISCUSSION

The Val Sorda sequence records several sedimentological and pedological processes that reflect different palaeoclimatic conditions during the upper Pleistocene. The base of the sequence (VS6) is composed of a thick (more than 10 m) glacial and fluvioglacial deposit, cemented at its base. According to Venzo (1957), Mancini (1960), Cremaschi (1987b), and Accorsi *et al.* (1990), this unit originated during the penultimate glacial event.

On the top of unit VS6, the rubefied paleosol is preserved only as a Bt-horizon (VS5). The upper part has been truncated, testifying to an erosional event. The clay mineral spectrum is quite different from the underlying till, differing by the lack of smectite and the presence of a dioctahedral vermiculite in large quantities. The dioctahedral nature of the vermiculite reflects stronger weathering compared to the loess sequence. It is generally accepted that trioctahedral minerals (containing Mg and Fe) are more sensitive to chemical weathering in contrast to the more stable dioctahedral minerals (containing Al). Transformation of smectite to vermiculite during pedogenesis is difficult to explain. The strongly weathered soft pebbles, consisting of vermiculite, could have influenced the whole clay mineral composition of the soil horizon, alternatively, vermiculite clays could have been illuviated from upper horizons of the paleosol that were subsequently eroded. The heavy mineral spectrum, with high amphibole content and traces of this mineral in the bulk sample, could be indicative of only

slightly wheatering of the soil horizon, and thus the vermiculite should be originated from the strongly weathered pebbles from the till. Nevertheless, amphiboles are not detectable in the clay fraction, carbonates are leached, and illuvial clay and high iron and manganese concentration are well expressed in the paleosol, suggesting strong weathering. In addition, the enhancement of magnetic susceptibility is striking, being more than two times higher than in interstadial paleosols. The formation of this soil type requires a seasonally contrasted warm climate and humid periods during a long time span; these conditions only occur during interglacial periods. As the interglacial paleosol is occurring between sediments of the penultimate glacial stage and the last glacial stage, it can be attributed to the Eemian interglacial (isotopic substage 5e).

On the top of the Eemian paleosol, a reworked layer was deposited (VS4), which shows characteristics of both underlying and overlying units. The unit VS4 is an admixture of the underlying paleosol and the overlying loess, as is recorded by the clayey-sandy texture, clay mineralogy, and a heavy mineral composition that is similar to the overlying loess unit. Field and micromorphological evidence indicate that soil material of the underlying paleosol is incorporated in the layer VS4. In particular, the high magnetic susceptibility values reflect components of the underlying rubefied paleosol (VS5).

The regular stone line at the top of the reworked layer confirms that it has been transported by colluvial processes, which indicates a climatic degradation towards cold and wet

conditions. As this layer is intercalated between the Eemian paleosol (VS5) and the Middle Pleniglacial loess unit (VS3, age control discussed below), its age cannot be determined exactly. For this period of transportation and accumulation, an Early Pleniglacial age as well as a Middle Pleniglacial age is possible.

Following the period of landscape instability and sediment reworking that created unit VS4, loess accumulation dominated, resulting in unit VS3. The lowermost loess layer contains pedorelicts and, locally, small rounded rock fragments indicative of continued colluvial phenomena, which we consider related to more humid climate episodes.

On the top of the reworked loess material, the formation of a Chernozem paleosol indicates a phase of relative climatic stability, which we relate to a continental cold and dry environment (steppe climate), when loess deposition was reduced relative to rates of pedogenesis. Following formation of the basal Chernozem, loess accumulation continued, but was interrupted by two phases of soil formation resulting in Chernozem-like paleosols. Therefore, we conclude that periods of loess deposition alternated with three stable phases of interstadial pedogenesis under steppe climate. We propose that the main loess accumulation phase is recorded in VS3 between 180 and 470 cm, as indicated by the maximum content of the heavy minerals epidote and garnet, the grain size dominated by silt, and the high amounts of unweathered primary chlorite in the clay fraction.

This pedological and paleoclimatic interpretation is supported by the palaeobotanical reconstruction proposed by Accorsi *et al.* (1990) for the Val Sorda sequence. Pollen analysis of the Chernozem horizons reflects a steppe environment, with *Graminae* and *Cichoriaceae* species dominant throughout the sequence. Arboreal pollen is scarce, but some *Pinus* and *Betula* occur. These vegetal associations suggest a dry and cold climate, with some warming evident by the appearance of *Quercus*. The palaeobotanical reconstruction of Val Sorda fits with the reconstruction of the whole Venetian Pre-Alps area proposed by Cattani (1990), who suggested an arid steppe that changed to steppe grassland during periods with a slight increase in temperature and humidity during the Pleniglacial.

The first (uppermost) Chernozem displays the strongest morphological expression of the three interstadial paleosols in the sequence; this observation is supported by characteristics such as color and magnetic properties. A radiocarbon age of 27,880 ± 600 years BP (Cremaschi *et al.*, 1987) places the soil formation during a late phase of the Middle Pleniglacial (isotopic stage 3), which may correspond to the Denekamp–Interstadial north of the Alps (Behre and van der Plicht, 1992). The underlying loess layer provided an OSL age of 36,000 ± 5,000 years BP (Accorsi *et al.*, 1990). We interpret the second and third Chernozem profiles to most probably represent the two older Middle Pleniglacial interstadials or even Early Pleniglacial

interstadials. Better age control is necessary, however.

On the top of the uppermost Chernozem paleosol, the deposition of laminated layers (VS2) suggests rapid and abrupt changes and, perhaps, faster deposition rates, linked to the approach of the ice sheet. The white finely laminated layer (VS2/105–109 cm) is very compact, inclined approximately to the eastern direction of the section, and shows field and microscopic evidence of high pressure and deformation. Thus, we attribute its formation to reworking of the top of the loess sequence by the overthrusting glacier and deposition by melt waters of the glacier. The reworked loess is covered by fluvioglacial sediments originating from the readvancing glacial front. These sediments were buried by the youngest till of the study area, which is referred to as the Solferino stage of the Upper Pleniglacial (isotope stage 2) (Cremaschi, 1987b).

The upper Pleistocene Val Sorda section is in part comparable to sequences north of the Alps. As in several loess-paleosol sequences in middle Europe, the Eemian paleosol is strongly developed as an intensively rubefied Bt-horizon and its upper horizons have been truncated (*cf.* Semmel, 1968; Ricken, 1983; Bibus, 1989; Bibus, 1996; Terhorst *et al.*, 2001). Even though the age of the redeposited material on top of the interglacial Bt-horizon is unknown, it is similar to other loess profiles. In Austria, a colluvial layer in a similar stratigraphic position comprises a time span from the Early to late Middle Pleniglacial (Terhorst *et al.*, 2002). Only the upper part of VS3, corresponding to the uppermost Chernozem and its parent material, can be reliably correlated with Middle European loess sequences because of the two numerical ages. Based on the sedimentation age (OSL) of 36,000 ± 5,000 years BP (Accorsi *et al.*, 1990) and the age of the soil formation at about 27,880 ± 600 years BP (Cremaschi *et al.*, 1987), we correlate the uppermost Chernozem with the Denekamp–Interstadial. In areas north of the Alps, such as in the Alpine foreland or the Rhine–Main area, this interstadial period is recorded by a weakly expressed brown soil (the Lohner Soil) interpreted to have formed in a cold arctic climate. The difference in morphological expression between the Val Sorda Chernozem and the Lohner Soil allows us to propose that the climatic gradient between areas north and south of the Alps must have been greater than present.

CONCLUSIONS

The Eemian paleosol at Val Sorda shows evidence of carbonate leaching, clay illuviation, and other interglacial scale pedogenic processes representative of a warm and seasonal climate. In contrast, in the three Chernozem profiles formed in isotope stage 3, loess express weak pedogenic organization, namely bioturbation and recalcification features, along with no evidence of mineral weathering, which we interpret as interstadial pedogenesis under a steppe climate. The interpretation proposed here agrees with recent

works on the Val Sorda sequence (Cremaschi, 1987b; Accorsi *et al.*, 1990), although in this work we recognize the three buried Chernozem paleosols in the main loess unit. We correlate the upper most Chernozem with the Lohner Soil that occurs north of the Alps.

Loess is generally characterized by enhanced values of magnetic susceptibility, while glacial sediments show reduced values. Interstadial paleosols are poorly discriminated from loess by magnetic susceptibility, whereas the Eemian paleosol shows a significant peak, presumably correlated to the *in situ* formation of ultrafine magnetic minerals (Maher, 1998). Despite this, ultrafine superparamagnetic ferrimagnetic mineral grains (magnetite) are present with maximum values in the two upper Chernozem paleosols and in particular in the rubefied paleosol and its overlying colluvial layer. For this reason (Dearing *et al.*, 1997; Maher, 1998), the conclusion is that the presence of ultrafine (SP) minerals is due to pedogenic processes, and that they give a more sensible parameter for interstadial soil formation in the study area than magnetic susceptibility can provide (Kukla *et al.*, 1988).

Overall, the Val Sorda sequence preserves a very complex palaeoenvironmental record of landscape evolution during the upper Pleistocene in northern Italy. Further age control is necessary to fully understand the chronology of sedimentation and soil formation, in addition to correlation with other European loess sequences.

ACKNOWLEDGMENTS

REFERENCES

Accorsi, C.A., Baroni, C., Cremaschi, M., Filippi, N., Maggi, V., Magnani, P., Nisbet, R., 1990, The loess in Appenine Fringe, *in* Cremaschi, M. (ed.), The Loess in Northern and Central Italy; a Loess Basin Between the Alps and the Mediterranean Region: Milano, Quaderni di Geodinamica Alpina e Quaternaria, 1, 73–101.

Behre, K.E., van der Plicht, J., 1992, Towards an absolute chronology for the glacial period in Europe; radiocarbon dates from Oerel, northern Germany: Vegetation History and Archaeobotany, 1, 111–117.

Bibus, E. (ed.), 1989, Paläoböden im mittleren Neckarbecken unter besonderer Berücksichtigung von Lößstratigraphie und Paläoböden, Exkursionsführer, 8. Tagung des Arbeitskreises "Paläoböden" der Deutschen Bodenkundlichen Gesellschaft: Heilbronn, 31 p.

Bibus, E., 1996, Äolische Deckschichten, Paläoböden und Mindestalter der Terrassen in der Iller-Lech-Platte: Geologica Bavarica, 99, 135–164.

Bullock, P., Fedoroff, N., Jongerius, A., Stoops, G., Tursina, T., Babel, C., 1985, Handbook for Soil Thin Section Description: Albrighton, Waine Research Publication, 152 p.

Brindley, G.W., Brown, G., 1980, Crystal Structures of Clay Minerals and their X-Ray Identification: London, Mineralogical Society, 495 p.

Cattani, L, 1990, Steppe environments at the margin of the Venetian Pre-Alps during the Pleniglacial and Late-Galcial periods, *in* Cremaschi, M. (ed.), The Loess in Northern and Central Italy; a Loess Basin between the Alps and the Mediterranean Region: Quaderni di Geodinamica Alpina e Quaternaria, 1, 133–137.

Chiesa, S., Coltorti, M., Cremaschi, M., Ferraris, M., Floris, B., Prosperi, L., 1990, Loess sedimentation and quaternary deposits in the Marche Province, *in* Cremaschi, M. (ed.), The Loess in Northern and Central Italy; a Loess Basin between the Alps and the Mediterranean Region: Quaderni di Geodinamica Alpina e Quaternaria, 1, 103–130.

Cremaschi, M., 1987a, Loess deposits of the Plain of the Po and of the adjoining Adriatic basin (Northern Italy), *in* Pécsi, M., French, H.M. (eds.), Loess and Periglacial Phenomena: Budapest, Akadémiai Kiadò, 125–140.

Cremaschi, M., 1987b, Paleosols and Vetusols in the Central Po Plain (Northern Italy); A study in Quaternary Geology and Soil development: Milano, Unicopli, 316 p.

Cremaschi, M. (ed.), 1990a, The Loess in Northern and Central Italy; a Loess Basin between the Alps and the Mediterranean Region: Quaderni di Geodinamica Alpina e Quaternaria, 1, 187 p.

Cremaschi, M., 1990b, Sedimentazione loessica nel Bacino Padano-Adriatico durante il Pleistocene Superiore: Memorie della Società Geologica Italiana, 45, 843–856.

Cremaschi, M., Alessio, M., Allegri, L., Azzi, C., Calderoni, G., Cortesi, C., Petrone, V., Spezzi-Bottiani, C., 1987, Una data radiocarbonica del paleosuolo su loess incluso nella successione stratigrafica della Val Sorda (sistema morenico del Garda): Rendiconti della Società Geologica Italiana, 10, 29–32.

Dearing, J.A., Bird, P.M., Dann, R.J.L., Benjamin, S.F., 1997, Secondary ferrimagnetic minerals in Welsh soils: a comparison of mineral magnetic detection methods and implications for mineral formation: Geophysical Journal International, 130, 727–736.

Durn, G., Ottner, F., Slovenec, D., 1999, Clay minerals as an indicator of polygenetic origin of Terra Rossa in Istria, Croatia: Geoderma, 91 (1-2), 125–150.

Fraenzle, O., 1965, Die Pleistozäne Klima und Landschaftsentwicklung der nördlichen Po-Ebene im Lichte bodengeographischer Untersuchungen: Akademie der Wissenschaften und der Literatur in Mainz, Abhandlungen der Mathematisch-Naturwissenschaftliche Klasse 8, 336–456.

Gale, S.J., Hoare, P.G., 1991, Quaternary Sediments: New York, Belhaven Press, 323p.

Hodgson, J.M. (ed.), 1976, Soil Survey Field Handbook; Describing and Sampling Soil Profiles: Harpenden, Soil Survey of England and Wales, Soil Survey Technical Monograph, 5, 99 p.

Kukla, G., Heller, F., Liu, X.M., Xu, T.C., Liu, T.S., An, Z.S., 1988, Pleistocene climates in China dated by magnetic susceptibility: Geology, 16, 811–814.

Maher, B., 1998, Magnetic properties of modern soils and Quaternary loessic paleosols: paleoclimatic implications: Palaeogeography, Palaeoclimatology, Palaeoecology, 137, 25–54.

Mancini, F., 1960, Osservazione sui loess e sui paleosuoli dell'Anfiteatro orientale del Garda e di quello di Rivoli Veronese: Atti della Società Italiana Scienze Naturali, 99, 221–250.

Mange, M.A., Maurer, H.F.W., 1992, Heavy Minerals in Colour: London, Chapman & Hall, 147 p.

Moore, D.M., Reynolds, R. C. Jr., 1997, X-Ray Diffraction and the Identification and Analysis of Clay Minerals: New York, Oxford University Press, 378 p.

Nicolis, E., 1899, Triplice estensione glaciale ad Oriente del Lago di Garda: Atti del Regio Istituto Veneto di Scienze, Lettere ed Arti, 58 (2), 316–319.

Parfenoff, A., Pomerol, C., Tourenq, J., 1970, Les minéraux en grains: Paris, Masson et C.ie Editeurs, 578+21 p.

Ricken, W., 1983, Mittel- und jungpleistozäne Lößdecken im südwestlichen Harzvorland; Stratigraphie, Paläopedologie und

Konnektierung in Flußterrassen: Catena, 3, 95–138.

Semmel, A., 1968, Studien über den Verlauf jungpleistozäner Formung in Hessen: Frankfurter Geographische Hefte, 45, 1–133.

Stoops, G., 1998, Key to the ISSS "Handbook for Soil Thin Section Description": Natuurwetenschappelijk Tijdschrift, 78, 193–203.

Terhorst, B., Ottner, F., 2003, Polycyclic Luvisols in Northern Italy: Palaeopedological and Clay Mineralogical Characteristics: Quaternary International, 106/107, 215–231

Terhorst, B., Appel, E., Werner, A., 2001, Results of paleopedological and magnetic susceptibility analyses in a loess exposure in SW-Germany: Quaternary International, 76/77, 231–240.

Terhorst, B., Frechen, M., Reitner, J., 2002, Chronostratigraphische Ergebnisse aus Lößprofilen der Inn- und Traun-Hochterrassen in Oberösterreich: Zeitschrift für Geomorphologie, Neue Folge, Supplementbände, 127, 213–232.

Venzo, S., 1957, Rilevamento geologico dell'anfiteatro morenico frontale del Lago di Garda. Parte I: Tratto occidentale Gardone-Desenzano: Memorie della Società Italiana Scienze Naturali, 2 (2), 73–140.

Venzo, S., 1961, Rilevamento geologico dell'anfiteatro morenico del Garda. Parte II: Tratto orientale Garda-Adige ed anfiteatro atesino di Rivoli Veronese: Memorie della Società Italiana Scienze Naturali, 14 (1), 82 p.

Walden, J., Olfield, F., Smith, J.P., 1999, Environmental Magnetism: a practical guide: London, Quaternary Research Association, Technical Guide No. 6, 250 p.